

Studies on chromophore coupling in isolated phycobiliproteins

III. Picosecond excited state kinetics and time-resolved fluorescence spectra of different allophycocyanins from *Mastigocladus laminosus*

Alfred R. Holzwarth,* Edith Bittersmann,* Wolfgang Reuter,† and Werner Wehrmeyer†

*Max-Planck-Institut für Strahlenchemie, D-4330 Mülheim a.d. Ruhr; and †Fachbereich Biologie-Botanik, Philipps-Universität Marburg, Lahnberge, D-355 Marburg/Lahn, Federal Republic of Germany

ABSTRACT The excited state kinetics of three different allophycocyanin (AP) complexes has been studied by picosecond fluorescence spectroscopy. Both the fluorescence kinetics and the decay-associated fluorescence spectra of the different complexes can be understood on the basis of a structural model for AP which uses (a) an analogy to the known x-ray determined structure of C-phycocyanin, (b) the biochemical analogies of AP and C-phycocyanin, and (c) the biochemical composition of AP-B (AP-681). A model is developed that describes the excited state kinetics as a mixture of

internal conversion processes within a coupled exciton pair and energy transfer processes between exciton pairs. We found excited state relaxation times in the range of 13 ps (AP with linker peptide) up to 66 ps (AP-B). The trimeric aggregates AP 660 and AP 665 show one fast relaxation component each, as was expected on the basis of their symmetry properties. The lower symmetry of AP-B (AP-681) gives rise to two fast lifetime components ($\tau_1 = 23$ ps and $\tau_2 = 66$ ps) which are attributed to internal conversion and/or energy transfer between excitonic states formed by the coupling of sym-

metrically and spectrally nonequivalent chromophores. It is proposed that the internal conversion between exciton states of strongly coupled chromophores fulfills the requirements of the small energy gap limit. Thus, internal conversion rates in the order of tens of picoseconds are feasible. The influence of the interaction of the linker peptide on the properties of the AP trimer are manifested in the fluorescence kinetics. Lack of the linker peptide in AP 660 gives rise to a heterogeneity in the chromophore conformations and chromophore-chromophore interactions.

INTRODUCTION

Allophycocyanin (AP)¹ is one of the phycobiliproteins which forms the building blocks of the so-called phycobilisomes (PBS) which function as accessory light-harvesting complexes in cyanobacteria (blue-green algae) and red algae. Allophycocyanin(s) are located in the core of the PBS while the rodlike structures which are attached to the core in a radial manner contain the phycobiliproteins phycocyanin and sometimes phycoerythrin or phycoerythrocyanin (for review of PBS structure see references 2, 3). A basic characteristic of phycobiliproteins is the fact that they contain two or more groups of spectrally and sometimes also chemically different chromophores (4). The excited state relaxation and ground state recovery kinetics have been studied for several isolated phycobiliproteins using picosecond fluorescence and picosecond absorption techniques, respectively (for recent reviews see references 5, 6).

We have recently presented a detailed kinetic fluores-

cence study of the phycobiliprotein C-phycocyanin (C-PC) as a function of its aggregation state (7, 8). It has been shown there how the symmetry properties of C-PC, as determined from the x-ray structure (9, 10) greatly simplify the theoretically observable fluorescence kinetics. These results, together with picosecond data from intact PBS have been used to develop a kinetic model which provides for the detailed understanding of the energy transfer processes within PBS rods and from the rods to the core (11). In contrast to that our understanding of the energy transfer kinetics and pathways between the AP-aggregates within the PBS core is much less detailed. Therefore, the present study of isolated APs is intended as a step towards a better understanding of the energy transfer processes in the PBS core. AP is the simplest phycobiliprotein, carrying one chromophore only at each of the protein subunits α and β . Furthermore, because C-PC and AP bear many similarities both with regard to their chromophores as well as their apoproteins (12, 13), the comparison of kinetic data of the more simple AP with those of C-PC should allow for a further check of some of the conclusions drawn earlier (7). Recently, a detailed biochemical and spectral study of various AP complexes from *Mastigocladus* has been published (14). The corresponding allophycocyanin com-

A preliminary account of this work has been presented at the Workshop on Organization and Function of Photosynthetic Antennas, Freising, 1987 (1).

¹Abbreviations used in this paper: AP, allophycocyanin; C-PC, C-phycocyanin; DAS, decay-associated spectrum; F, fluorescing; IC, internal conversion; PBS, phycobilisome(s); S, sensitizing.

plexes from *Synechococcus 6301* had been characterized earlier (15, 16).

A result common to all of the isolated phycobiliproteins studied in detail so far by time-resolved techniques was the observation of kinetic components with lifetimes in the range of tens of picoseconds (5, 6). These short-lived components have been interpreted in terms of energy transfer between the different types of chromophores. Such an interpretation is based on the assumption of a very weak coupling between chromophores so that Förster resonance theory could be applied. Theoretical calculations based on the Förster mechanism gave at least partial agreement with experimental data for C-PC (17). However, recent estimates of the coupling energy V between pairs of close-lying chromophores in C-PC gave values for V ranging up to 100 cm^{-1} (18–20). If these values are correct, theories appropriate for intermediate or even strong coupling will have to be applied. In this case the short-lived kinetic components could no longer be regarded as mere energy transfer components and a new interpretation of the experimental data would be required. We thus propose an alternative model which accounts for the fast kinetic components also in the case of intermediate to strong coupling.

MATERIALS AND METHODS

Allophycocyanin samples

Three different AP complexes have been isolated from the PBS of the cyanobacterium *Mastigocladus*. The detailed description of the isolation procedures as well as the biochemical characterization of these complexes will be published elsewhere (Reuter, W., and W. Wehrmeyer, submitted for publication). According to this characterization the AP complexes studied here are (a) a trimeric complex free of linker peptides with a composition $(\alpha_3^{\text{AP}}\beta_3^{\text{AP}})$ which will be called AP 660 according to its fluorescence emission maximum at 660 nm; (b) a trimeric complex called AP 665 with a 10-kD (apparent molecular weight) linker peptide of composition $(\alpha_3^{\text{AP}}\beta_3^{\text{AP}})L_c^{10}$; and (c) an allophycocyanin B heterotrimer with linker peptide of composition $(\alpha^{\text{APB}}\alpha_2^{\text{AP}}\beta_3^{\text{AP}})L_c^{10}$ called AP 681. Here, the superscripts AP and APB denote the subunits and chromophores of allophycocyanin and allophycocyanin B, respectively, while L_c denotes a linker peptide of the AP core. The exact molecular weight of this linker peptide has been determined by Füglistaller et al. (14) to be 8.9 kD by its amino acid composition.

The phycobiliprotein complexes were dissolved in potassium phos-

phate buffer (200 mM) of pH = 7.0 and contained 0.004% wt/vol sodium azide. All measurements were carried out at ambient temperature within one day after the isolation of the sample. The samples were neither frozen nor subjected to ammoniumsulfate precipitation at any time during or after the isolation.

Spectroscopic methods

Absorption spectra were measured on a spectrophotometer (model U 3200, Hitachi Ltd., Tokyo). Corrected fluorescence spectra were recorded on a computer-controlled luminescence spectrometer (Fluorolog, Spex Industries, Inc., Edison, NJ) as described previously (21). The steady-state absorption and fluorescence spectra have been deconvoluted into Gaussian components using a home-written spectra analysis program based on the Levenberg-Marquardt algorithm (IMSL Library, Houston, TX) according to a least-squares criterion (22, 23). The circular dichroism spectra have been measured on a CD-spectrometer (JASCO, Japan). The spectra presented have been corrected for the nonflat baseline. The band positions of the absorption, fluorescence, and CD spectra are compiled in Table 1. The spectra for the three AP complexes are given in Figs. 1–3.

Picosecond fluorescence decays and decay-associated (time-resolved) fluorescence spectra were measured as described previously (7) on a single-photon timing apparatus with ~5 ps resolution by deconvolution with the apparatus response of ~50 ps halfwidth. All measurements were carried out under magic angle polarization (isotropic fluorescence) conditions to eliminate the interference with time-dependent anisotropy effects. The various sets of decay curves were analyzed by a global data analysis procedure as described (7) (sometimes also called "simultaneous" analysis procedure). The underlying kinetic model for the fluorescence kinetics $F(t)$ as a function of the excitation (λ_{exc}) and emission (λ_{em}) wavelength was

$$F(t, \lambda_{\text{exc}}, \lambda_{\text{em}}) = \sum_{i=1}^n A_i(\lambda_{\text{exc}}, \lambda_{\text{em}}) \cdot \exp(-t/\tau_i). \quad (1)$$

A plot of the amplitude $A_i(\lambda_{\text{exc}}, \lambda_{\text{em}})$ as a function of the emission wavelength λ_{em} represents a decay-associated emission spectrum (DAS) for the kinetic component i . A positive amplitude represents a decay term and a negative amplitude a rise term. The latter indicates an indirect population of chromophores and/or excited states due to a transition between different types of excited chromophores and/or states. The shape of the decay-associated spectrum will in such a case be given by the weighted difference emission spectra of the donor and acceptor fluorescence (see reference 7 and Kinetic Analysis below).

RESULTS

Steady-state spectra

The results of the Gaussian deconvolution of the absorption and fluorescence spectra of the three AP complexes

TABLE 1 Positions of the absorption, fluorescence emission, and circular dichroism bands (nanometers) of the three allophycocyanin complexes in phosphate buffer, pH = 7.0 at room temperature

Sample	$\lambda_{\text{max}}^{\text{abs}}$	$\lambda_{\text{max}}^{\text{em}}$	λ^{CD}
$(\alpha_3^{\text{AP}}\beta_3^{\text{AP}})$; (AP 660)	652	660 ($\lambda_{\text{exc}} = 635 \text{ nm}$)	656(max), 625(max)
$(\alpha_3^{\text{AP}}\beta_3^{\text{AP}})L_c^{10}$; (AP 665)	653	665 ($\lambda_{\text{exc}} = 635 \text{ nm}$)	656(max), 633(min), 595(min)
$(\alpha^{\text{APB}}\alpha_2^{\text{AP}}\beta_3^{\text{AP}})L_c^{10}$; (AP 681)	655	681 ($\lambda_{\text{exc}} = 630 \text{ nm}$)	670(max), 598(min)

*The errors in maxima are $\pm 1 \text{ nm}$.

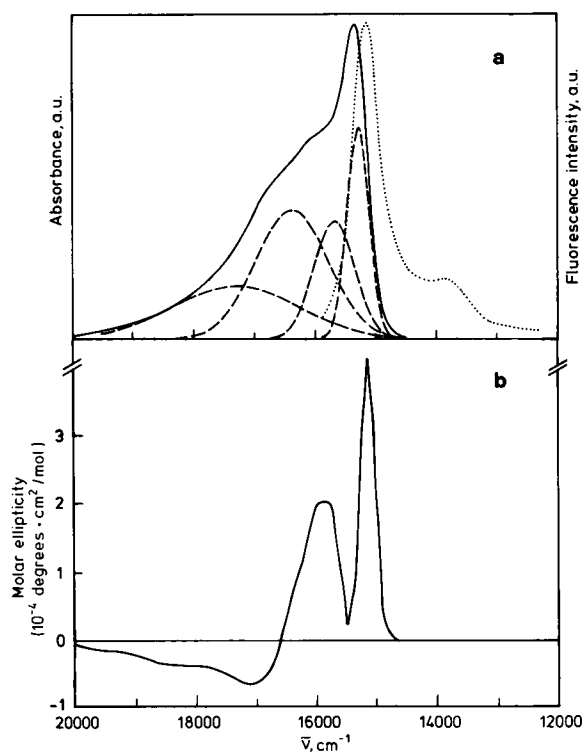


FIGURE 1 Steady-state spectra of AP 660. (a) Absorption (solid line) and fluorescence emission (dotted line). Also shown are the results of the Gaussian deconvolution of the absorption into four components (dashed line) (c.f. Table 2). (b) Circular dichroism spectrum.

(Figs. 1–3) are compiled in Table 2. The deconvolution has been carried out for the spectra plotted on a scale linear in wave numbers $\tilde{\nu}(\text{cm}^{-1})$. Although their absorption maxima are only slightly different, the AP complexes differ greatly both with respect to the shape of their absorption spectra and also in their CD spectra. For AP 660 and AP 665 four Gaussian components proved to be necessary and sufficient for a good description of the absorption in the range 14,400–19,500 cm^{-1} . For AP 681 five components were necessary. These deconvoluted absorption spectra of the three complexes should be compared for conservative elements in their components, i.e., for spectral components that are similar or identical with respect to band position and/or halfwidths for the three complexes.

In each case the two shortest-wavelength components in the absorption spectra with large halfwidths seem to describe the diffuse vibrational structure of the spectra while the much narrower long-wavelength Gaussian bands describe the 0–0 transitions. For this reason only the latter components are relevant for our analysis of the absorption maxima of the different chromophores and/or transitions. The absorption and CD spectra of the three

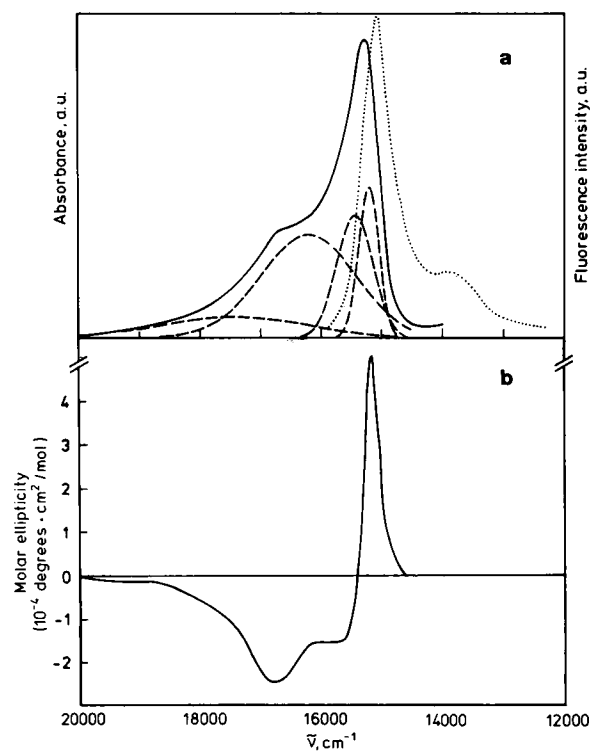


FIGURE 2 Steady-state spectra of AP 665 (see Fig. 1 caption for explanation of symbols).

complexes are very similar to those reported (14), except for a larger positive band of AP 681 in our CD spectrum at ≈ 670 nm.

Decay-associated spectra

The decay-associated emission spectra (DAS) with picosecond time resolution were measured for all three AP complexes at different excitation wavelengths. Fluorescence decays were recorded at 10-nm intervals as a function of the emission wavelength. The complete set of decay curves from each trimer was subjected to a global deconvolution procedure. The residual plots and autocorrelation functions for a single-exponential and a double-exponential model function for the fluorescence decays of AP 665 are shown in Fig. 4. Comparison of these plots indicates clearly the necessity for a double-exponential model to describe the kinetic data properly. The single-exponential fit results in large systematic deviations in the residuals around the maximum of the decay curve and also in the autocorrelations. In contrast, the residual plots (Fig. 5) and autocorrelation functions indicate that for AP 681 at least three exponentials are required for a good fit.

The decay-associated spectra for the three AP com-

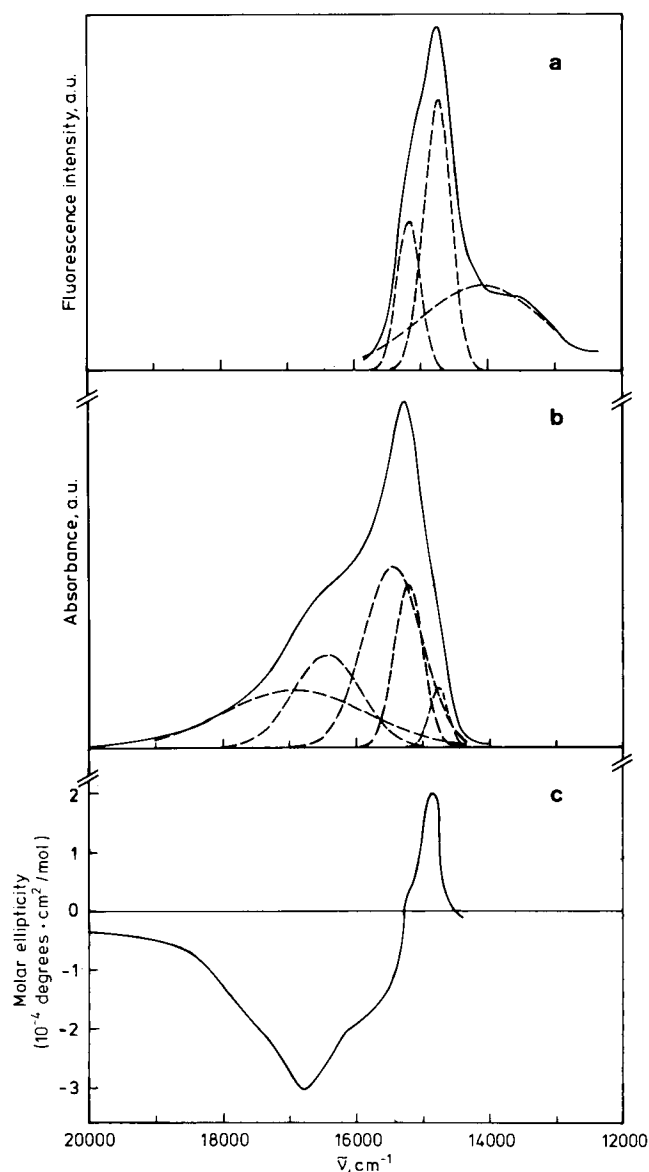


FIGURE 3 Steady-state spectra of AP 681. (a) Experimental fluorescence spectrum (solid line) ($\lambda_{\text{exc}} = 620$ nm) and its Gaussian deconvolution into three components (dashed line). (b) Absorption spectrum (solid line) and Gaussian deconvolution into five components (dashed line) (c.f. Table 2). (c) Circular dichroism spectrum.

plexes calculated by the global analysis procedure are given in Fig. 6, A–C. The corresponding component lifetimes obtained from the global analysis are collected in Table 3. The excitation wavelength for AP 660 and AP 665 was chosen to be 620 nm (data not shown) and 635 nm (Fig. 6, A and B), i.e., slightly shorter than the maximum of the second absorption band from the Gaussian deconvolution (c.f. Table 2). AP 681 was excited at

TABLE 2 Results of the Gaussian deconvolution of the absorption spectra of three different AP forms

Sample	Component	Amplitude*	FWHM [†]		Position [‡]
			cm^{-1}	cm^{-1}	
AP 660 (absorption)	1	1.0	430	15295	(653.8)
	2	0.56	790	15670	(638.2)
	3	0.60	1410	16366	(611.0)
	4	0.25	2460	17298	(578.1)
AP 665 (absorption)	1	1.0	400	15210	(657.5)
	2	0.81	700	15440	(647.6)
	3	0.68	1830	16200	(617.3)
	4	0.14	2860	17388	(575.1)
AP 681 (absorption)	1	0.33	330	14773	(676.9)
	2	0.903	510	15219	(657.1)
	3	1.0	1030	15467	(646.5)
	4	0.52	1200	16436	(608.4)
	5	0.32	2520	16923	(590.9)
AP 681 (fluorescence)	1	0.55	400	15124	(661)
	2	1.0	490	14684	(681)
	3	0.31	2200	14039	(712)

The deconvolution data of the APC 681 fluorescence emission spectrum is also given.

*Amplitudes are normalized to the largest component.

[†]Full width at half maximum.

[‡]Numbers in parentheses represent corresponding wavelength in nanometers.

620, 670 (data not shown), and 650 nm (Fig. 6 C), i.e., slightly shorter than the absorption maximum.

AP 660

The shortest-lived component of $\tau_1 = 25$ ps shows a positive amplitude (decay term) at short emission wavelengths (Fig. 6 A). At long wavelengths the corresponding DAS has a negative amplitude (rise term) and a broad spectral shape. The zero-crossing occurs around 655 nm, i.e., close to the absorption maximum. The appearance of a negative sign in the DAS of the 25-ps component identifies the respective process as a transition between spectrally different excited states. The two long-lived components of 720 and 1,700 ps have positive amplitude across the whole emission spectrum. They both have their wavelength maximum at 660 nm and very similar spectral shape but largely different amplitudes. The maximum of these two components coincides further with the maximum of the steady-state emission spectrum (Table 1).

AP 665

There are only two kinetic components present in this complex (Fig. 6 B). The short-lived one with $\tau_1 = 14$ ps

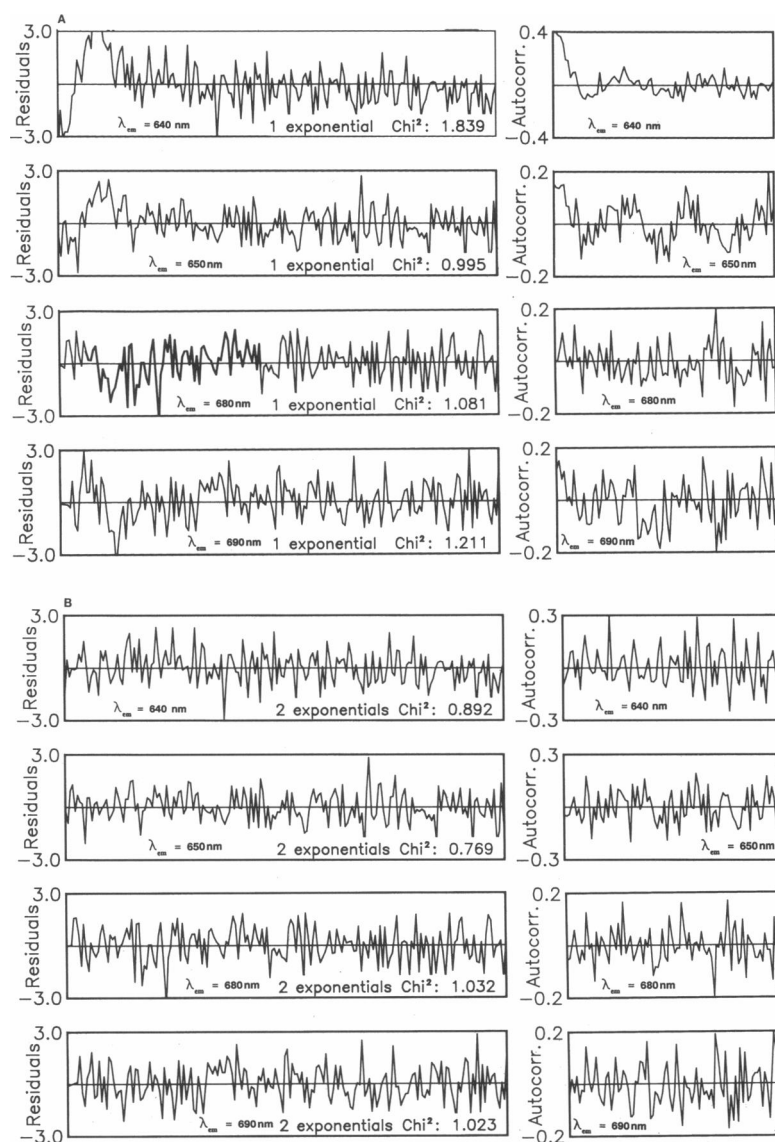


FIGURE 4 Residual plots and autocorrelation functions from the global fit to the decay data of AP 665 for a single-exponential (*A*) and a double-exponential (*B*) model function.

has positive amplitude at short wavelengths and negative amplitude at long wavelengths. The zero-crossing occurs near 660 nm. As compared to the corresponding DAS of AP 660 the bandwidth of the negative part is much narrower and its amplitude is larger. The long-lived component has only positive amplitude and shows a spectral maximum very close to that of the steady-state emission spectrum (665 nm) (Table 1). Similar lifetimes and spectra were also observed upon excitation at 620 nm. Upon excitation at 650 nm no short-lived emission component was present.

AP 681

The DAS of this complex contain two short-lived components ($\tau_1 = 23$ ps, $\tau_2 = 66$ ps), both of which show negative amplitude contributions. The $\tau_1 = 23$ ps component shows only a negative amplitude in the wavelength range accessible because a measurement closer to the excitation wavelength was not possible due to scattering problems. Their zero-crossing wavelengths (estimated for the $\tau_1 = 23$ ps component by extrapolation) differ by ~ 20 nm (Fig. 6 C). The third, long-lived component ($\tau_3 = 1,700$

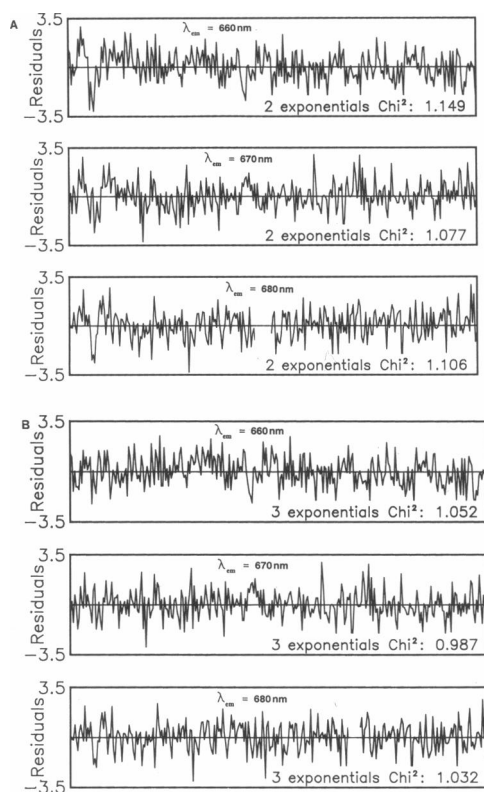


FIGURE 5 Residual plots from the global fit to the decay data of AP 681 for a double-exponential (A) and a three-exponential (B) model function.

ps) shows only positive amplitudes. The spectrum peaks at ~ 680 nm, again very close to the maximum of the steady-state emission and it also has a shoulder around 660 nm. Upon excitation at 620 nm similar lifetimes and spectra, although with different relative amplitudes, were obtained. At $\lambda_{\text{exc}} = 670$ nm the 66-ps component was not observed.

DISCUSSION

The α^{AP} and β^{AP} subunits of the different AP complexes carry one phycocyanobilin chromophore each at amino acid positions α -84 and β -84, respectively (12, 13, 24). The position of the phycocyanobilin chromophore of α^{APB} has been determined recently (25). According to this analysis α^{APB} is highly homologous to α^{AP} . Thus, in α^{AP} , α^{APB} , and β^{AP} the bilin chromophores are bound at the equivalent positions as in C-PC except for the β -155 chromophore which is absent in AP. The amino acid sequences of AP α - and β -subunits are highly homologous to the sequences of the corresponding C-PC subunits (12, 13). Therefore, similarities are expected in the folding of the respective polypeptide chains in AP and C-PC.

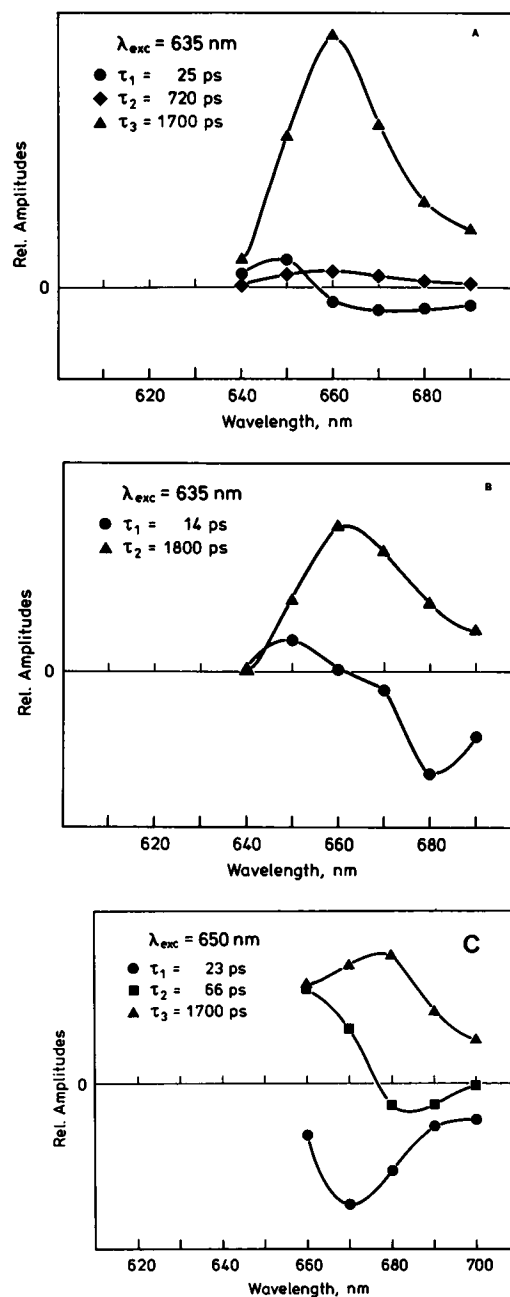


FIGURE 6 Decay-associated fluorescence spectra (c.f. Eq. 1) as calculated from the global fits to the decay curves of AP 660 (A), AP 665 (B), and AP 681 (C).

Electron microscopy of AP- and C-PC-trimers has shown furthermore that both pigments are disks with very similar dimensions (26). No x-ray structure data are available so far on AP. However, the far-reaching analogies between C-PC and AP may suggest similar tertiary and quaternary structures for the two protein complexes. We therefore are probably justified in assuming as a first

TABLE 3 Average fluorescence lifetimes (τ_i , ps) of the kinetic components of the AP complexes from *Mastigocladus laminosus*

Compound	λ_{exc}	τ_1^*	τ_2^*	τ_3^*
	nm			
AP 660	635	25 [‡]	720	1700
AP 665	635	14 [‡]	—	1800
AP 681	650	23 [‡]	66 [‡]	1700

Each set of lifetimes has been calculated from 5 to 12 fluorescence decays using the global data analysis procedure.

*Maximum errors in the short lifetimes are 10% or ± 3 ps, whichever is larger. For the long lifetimes the maximum error is 5%.

[‡]Lifetime component also adopts negative amplitude values (rise term) at some emission wavelengths.

approximation at least the same symmetry properties and perhaps also similar relative chromophore orientations for AP as has been determined from the x-ray data for C-PC (9, 10). In fact, for the present analysis and interpretation of our kinetic data it will be entirely sufficient to assume the equivalent threefold symmetry axis (C_3 -symmetry) for AP 660 and AP 665 which is known for C-PC (9). Due to the presence of the APB chromophore the AP 681 complex is not expected to have such a high symmetry. In the following we shall first outline the possible chromophore coupling schemes, then analyze the excited-state kinetics in the highly symmetric AP 660 and AP 665 trimers and finally discuss the kinetics in the less symmetric AP 681. The schematic diagrams of the assumed structures of the trimeric APs and AP 681 (analogous to C-PC [9]) are given in Fig. 7, *A* and *B*, respectively.

Analysis of absorption and fluorescence spectra

From the assumed structures of AP 660 and AP 665 (see above) and the presence of two different types of chromo-

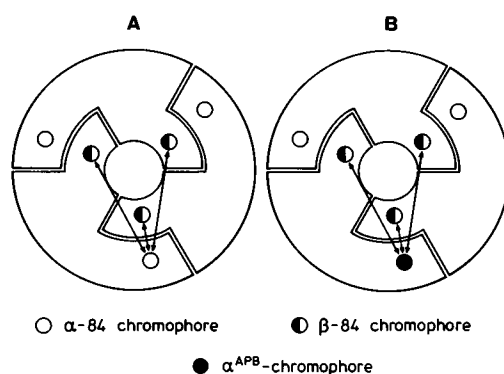


FIGURE 7 Schematic model of the assumed structure of AP trimers 660 and 665 (*A*) and of AP 681 (*B*).

phores we expect two absorption transitions in the long-wavelength band. These transitions should either be assigned directly to the two types of chromophores present in the trimers or to the two transitions in the exciton-coupled pairs. The exciton-coupled pairs are expected to be formed by the close lying pairs of α -84/ β -84-chromophores in different monomers (c.f. Fig. 7 *A*). The Gaussian deconvolution supports this hypothesis. For both AP 660 and AP 665 two relatively narrow absorption bands (components 1 and 2 in Table 2) were found in the deconvolution. These bands both undergo a bathochromic shift of some 85 cm^{-1} (component 1) and 170 cm^{-1} (component 2) upon association of the trimer with the linker peptide. We assign these bands to the two 0–0 transitions of the long-wavelength absorbing states and conclude from the fact that their respective halfwidths are very similar in the two complexes each, that these transitions do not reverse their relative positions upon association of the trimer with the linker peptide. The latter conclusion has been arrived at (14) on the basis of the assumption that the linker peptide does influence only β^{AP} and not α^{AP} . This assumption is possibly not justified if exciton coupling is substantial. It is worth mentioning that our Gaussian analysis yields very similar results as the analysis of Csatorday et al. (27). Some differences are present in the high energy part, however, which was described in terms of a chimeric Gaussian/Lorentzian band by Csatorday et al. (27). It is gratifying to see that the analysis finds two bands at exactly the same positions for AP 681 (components 2 and 3, Table 2) and AP 665 (components 1 and 2). Such behavior might be expected on the basis of the fact that one α^{AP} is exchanged against an α^{APB} subunit in AP 681 (c.f. Fig. 7 *B*). Also the somewhat increased bandwidths of these bands do not come unexpected in view of the presumably different coupling strength between α^{AP}/β^{AP} chromophores on the one hand and α^{APB}/β^{AP} chromophores on the other hand. In AP 681 a new long-wavelength band at 677 nm (component 1) is observed in addition which reflects the absorption of α^{APB} . In all three complexes the two short-wavelength bands have the largest halfwidth and their maxima do not show a clear trend. For these reasons we do not assign these components to specific transitions or chromophores. Presumably, they describe the composite of the higher vibronic transitions corresponding to the long-wavelength 0–0 transitions. We are well aware of the problems related to the Gaussian deconvolution of the spectra. Nevertheless, the clear trends and similarities provided by the comparison of the data of the three AP complexes make us confident that they provide a reasonably sound basis for our assignment given above.

We have not tried a similar deconvolution of the CD spectra because of the still larger uncertainties involved in their analysis as compared with that of the absorption

spectra. It seems to be clear, however, that the band positions found in the CD spectra, perhaps with the exception of the longest-wavelength CD band, do not directly reflect the transition energies found in the absorptions. It is more likely that a more complex relationship applies as analyzed in detail, e.g., for phycocyanin 612 (28).

The analysis of the fluorescence spectra of AP 660 and AP 665 resulted in two bands only which were congruent with the narrow band feature and the long-wavelength shoulder, i.e., the narrow band did not split into two Gaussian components. This was the case, however, for AP 681 (Fig. 3 *a*, Table 2). The two short-wavelength fluorescence bands correspond very well to the two long-wavelength absorption bands of this complex, exhibiting both a Stokes shift of 4–5 nm. Also this correspondence makes us confident that the Gaussian analysis of absorption and fluorescence spectra is meaningful in this case.

Chromophore–chromophore coupling

In the past the chromophore–chromophore interaction in phycobiliproteins has been discussed within the very weak dipole–dipole coupling model (see 5, 6, 29 for reviews). Consequently, the fast lifetime components have been interpreted as energy transfer components described by the Förster mechanism (7, 30–33). The Förster theory (34) can be applied only if the interaction energy is negligible as compared with the bandwidth of the electronic transition which is in the order of several hundred cm^{-1} and if the energy transfer rate is small when compared with the vibrational relaxation processes (35–37). Theoretical calculations seemed to be at least in partial agreement with such a mechanism (17). In contrast, first proposals of intermediate-to-strong coupling between chromophores in phycobiliproteins have been made by Jung et al. (38) and MacColl et al. (27, 39). Recent attempts to estimate the pairwise interaction energy of close-lying chromophore pairs in C-PC gave values in the range of ~ 50 to 100 cm^{-1} (18–20). Such a large value is comparable with the vibronic bandwidth and would place the interaction at least into the intermediate if not the strong coupling range (35, 36). The excited states resulting from this kind of interaction would no longer be localized states, as in the case of very weak coupling, but would be delocalized over both chromophores of a coupled pair, which now form a kind of supermolecule. In this case we could no longer interpret the relaxation from the high energy states to the low energy states as a pure energy transfer process. Rather, upon excitation of the upper exciton state an internal conversion (IC) process to the lower exciton state would

occur. In principle this internal conversion process could be observed as a fast kinetic component.

It is important to note that in the absence of detailed information on the relative orientation of transition moments, coupling energies, etc., there exists no a priori experimental way to distinguish this internal conversion process from an energy transfer process. The important question which has to be asked is: At which rate does such an internal conversion process occur? Can the relaxation times of a few tens of picoseconds observed in phycobiliproteins (5, 6) be assigned to IC between exciton states? We may assume that IC rates between exciton states should in principle be describable by the same theories as internal conversion between excited states of large molecules (40, 41). In general, such IC processes occur in the subpicosecond time range but little is known about the rates of IC between exciton-coupled states. Subpicosecond relaxation would be too fast to explain the experimentally observed relaxation rates in phycobiliproteins and in such case we would be left with an unexplained discrepancy between the experimental fluorescence data on the one hand and theoretical expectations on IC rates on the other hand. There are important exceptions to the ultrafast IC relaxations, however. If the electronic energy gap between states is small, the IC rates may be very slow even in a large molecule, e.g., 0.01 ps^{-1} or even less (42, 43). Such a situation could be realized for the two exciton states formed by the chromophore pairs in phycobiliproteins. If we take the difference between the two longest wavelength components from the Gaussian analysis of the absorption spectra of AP 660 and AP 665 as the energy difference between the exciton states, the energy gaps would be 370 and 240 cm^{-1} , respectively. These values are small enough to put the internal conversion process into the limit of the small energy gap (42). Thus, it would not be unreasonable to assign lifetime components in the range of tens of picoseconds to such an internal conversion process. The actual situation in a phycobiliprotein is expected to be more complex, however. Some chromophores could be strongly coupled, while other more distant chromophore pairs in the same protein could be weakly coupled. Thus, in a more realistic situation pairs of exciton states would be weakly coupled to other exciton states, thereby giving rise to energy transfer processes between exciton states belonging to different chromophore pairs. This situation is depicted schematically in Fig. 8. A similar model as presented here has been developed independently by Csatorday et al. (44).

Kinetic analysis

With the assumption of C_3 symmetry for AP 660 and AP 665, the excited state kinetics in these AP trimers can be

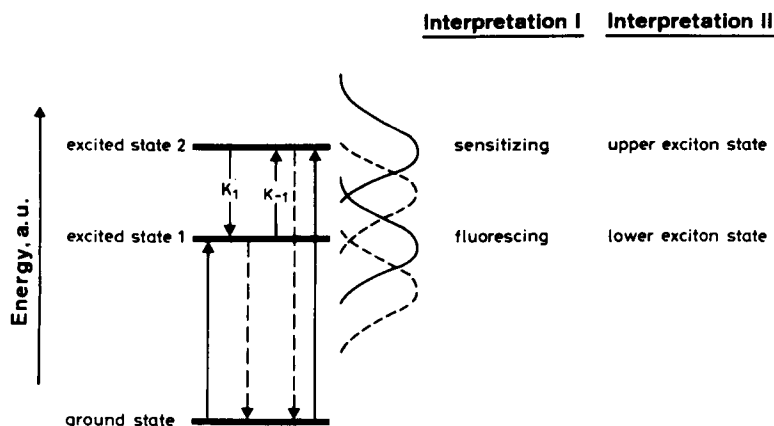


FIGURE 8 Energy scheme for the exciton coupling within AP 660 and AP 665. The rate constants k_1 and k_{-1} describe the transitions between the exciton states of one α -84/ β -84 chromophore pair and/or the energy transfer between sensitizing and fluorescing chromophores. In this paper interpretation II (strong coupling) for the excited states is proposed as the appropriate model. The Gaussian bands denote the absorption (*solid line*) and fluorescence (*dashed line*) spectra of the two exciton states.

treated as analogous to that of C-PC, which we have derived previously (7). The kinetic analysis is formally the same whether the weak coupling (interpretation I, Fig. 8) or the strong coupling model (interpretation II, Fig. 8), as discussed above, applies. Only the character of the excited states involved and thus the nature of the kinetic process described by the different rate constants are different. As compared with C-PC, the AP trimers are lacking one chromophore in each monomer. They therefore contain only two groups of identical chromophores/states instead of three as in C-PC. This feature simplifies the kinetic analysis substantially. In analogy to the extensive discussion presented for C-PC of symmetry properties and their influence on the formal kinetics (7), we have to consider for AP trimers two groups of interacting quasiparticles (pseudospecies or states). These quasiparticles are formed either by the excited states of the sensitizing (S) and fluorescing (F) (in case of weak coupling, interpretation I) or by the three pairs of exciton states of strongly coupled chromophores (interpretation II). Thus, applying the same formalism as in reference 7, we expect the fluorescence kinetics to be described theoretically by two exponential components. Using the derivation given in reference 7, we can directly write the analytical expression for the expected fluorescence kinetics and the decay-associated spectra. The fluorescence kinetics $d(\lambda_{em}, t)$ is given by

$$d(\lambda_{em}, t) = a_1(\lambda_{em}) \cdot \exp[-(k_r + k_{nr})t] + a_2(\lambda_{em}) \cdot \exp[-(k_{SF} + k_{FS})t] \quad (2)$$

Here k_r and k_{nr} denote the rate constants for radiative and nonradiative coupling of excited states to ground states, respectively. k_{SF} and k_{FS} are the overall rate constants of

transfer from S to F and from F to S chromophores, respectively, in the case of weak coupling. In the case of strong coupling, these rate constants are represented as a combination of the respective internal conversion rate constants between the two exciton states and of rate constants for weak interexciton state coupling. Note, e.g., that k_{SF} is the sum of all rate constants leading from one high-energy state to the three low-energy states in the trimer (7). The amplitudes $a_1(\lambda_{em})$ and $a_2(\lambda_{em})$ of the two kinetic components are the eigenvectors of the kinetic matrix and describe the experimental decay-associated spectra (cf. reference 7). They are given by

$$a_1(\lambda_{em}) = [\epsilon^S + \epsilon^F] \cdot [k_r^S e^S(\lambda_{em}) + k_r^F e^F(\lambda_{em})] + \frac{(k_{FS} - k_{SF})}{(k_{FS} + k_{SF})} \cdot \frac{1}{2} [k_r^S e^S(\lambda_{em}) - k_r^F e^F(\lambda_{em})] \quad (3)$$

$$a_2(\lambda_{em}) = \frac{k_{SF}\epsilon^S - k_{FS}\epsilon^F}{k_{SF} + k_{FS}} [k_r^S e^S(\lambda_{em}) - k_r^F e^F(\lambda_{em})]. \quad (4)$$

Here ϵ^S and ϵ^F are the extinction coefficients of the S and F chromophores, respectively, at the excitation wavelength, whereas e^S and e^F are the emission spectra of the S and F chromophores, respectively. Alternatively, for the strong coupling case, these variables denote the respective values for the exciton states.

It follows from these equations that kinetic component 1 will describe the radiative and nonradiative decay of the excited states to the ground state and it will be associated with a spectrum described by $a_1(\lambda_{em})$ that should be very similar to the steady-state emission spectrum. Component 2 describes the kinetic processes connecting the excited states and it will be associated with a spectrum given by $a_2(\lambda_{em})$ which is a weighted difference spectrum between

the fluorescence spectra of the S and F chromophores (in the case of weak coupling) and/or the upper and lower exciton states (in the case of strong coupling). For this reason, it contains positive and negative amplitudes. In the following discussion we shall only refer to the case of strong or intermediate coupling, as depicted in Fig. 8 (interpretation II). This is based on our belief that for AP and C-PC complexes in the trimeric or hexameric aggregation states, the evidence for intermediate-to-strong coupling is sound (19, 27, 39, 45). An experimental fact also supporting this interpretation consists in the large bathochromic absorption shift upon formation of the AP trimers from the monomers (39) which is difficult to explain otherwise.

Comparison with experimental data

The theoretical prediction of two fluorescence lifetime components is met by the experimental fluorescence kinetics of AP 665. We find a short-lived energy transfer component of $\tau_1 = 14$ ps and the expected long-lived component ($\tau_2 = 1.8$ ns). According to the kinetic equations given above, the τ_1 component represents the time required for the equilibration of the excitation energy between upper and lower exciton states. The relatively narrow bandwidths and large amplitudes of the positive and negative bands of the corresponding DAS (Fig. 6 B) indicate that the two emission bands are relatively narrow, which in turn means that the chromophore conformations and their relative orientations should be well defined (21, 46, 47) (c.f. reference 48 for review). The linker-free trimer AP 660 also shows one short-lived energy transfer component ($\tau_1 = 25$ ps). The basic interpretation for this component is the same as for the analogous one in AP 665. However, the longer lifetime indicates reduced relaxation rates. The reason for these reduced rates can be understood on the basis of the significantly different shapes and amplitudes of the corresponding DAS of the two trimers AP 660 and AP 665. The broad negative band in the DAS of decay component 1 in AP 660 indicates a very broad emission spectrum of the lower exciton state in that complex, in contrast to AP 665. This broad spectrum indicates a broad range of possible conformations and relative orientations of the chromophores, i.e., conformational heterogeneity. This can be understood as a kind of inhomogeneous broadening. The well-defined chromophore conformations in AP 665 therefore reflect the stabilizing interaction of the linker peptide on at least one of the chromophores, which is probably preferentially the β -84 chromophore situated next to the linker peptide in the central hole of the trimer. The absence of the linker peptide in AP 660 apparently introduces some heterogeneity into this protein complex.

This heterogeneity is further reflected by the presence of two long-lived lifetime components. If the chromophores of AP 660 were completely homogeneous and if it would fully satisfy the C_3 symmetry we should also observe only one long-lived component as in AP 665. Although the 720-ps component has a small amplitude it cannot be ignored and must be considered also as the manifestation of some chromophore and protein heterogeneity which probably mostly influences the spectroscopic properties of the β -84 chromophores. This situation is reminiscent of a similar observation which we have made earlier for C-phycocyanin (7). Also for the latter, only the aggregate that carried a linker peptide was found to be homogeneous. These observations seem to indicate that the linker peptides are an essential element for keeping the apoproteins and the chromophores of phycobiliproteins in their native conformation(s). Removal of the linkers probably introduces a more or less pronounced flexibility and deviations from native conformations.

It can be understood easily from Eq. 4 why upon excitation at 650 nm no short-lived component is observed in the DAS of AP 665. This excitation wavelength is situated between the maxima of the two long-wavelength absorption transition (Table 2) assigned to the lower and upper exciton states. Thus both states are excited with similar probability. More specifically, it is likely that at this wavelength $k_{SF}^S \approx k_{FS}^F$ thus leading to the value of the amplitude $a_2(\lambda_{em})$ close to zero. A similar situation probably holds for AP 681 with excitation at 670 nm where the 66-ps component disappears. Likewise in AP 681 upon excitation around 640 nm, the 66-ps component has negligible amplitude. We can also conclude from the deconvolution of the absorption spectra and from the wavelengths where the fast components in the DAS disappear that the absorption transitions from the ground state to the upper and lower exciton states have comparable size of transition moments. This in turn has significant consequences on the relative arrangements of the transition moments of the uncoupled chromophores.

In AP 681 the α -chain in one monomer is replaced by an α^{APB} -chain whose chromophore has different spectroscopic properties than that of α^{AP} . Thus, the C_3 symmetry is broken and a scheme like the one given in Fig. 7 B should apply. This lowering in symmetry makes the energy transfer kinetics much more complex. As far as the energy transfer and/or excited state relaxation processes are concerned we might be perhaps justified in assuming at least a symmetry plane perpendicular to the disc. In analogy to C-PC, this symmetry plane is of course not expected to apply to the apoprotein part (9). Assuming such a symmetry for the chromophore part only, we would expect either three or four lifetime components, based on the number of groups of symmetrically equivalent chromophores or excited states (7). At least two

components should represent transitions between different exciton states. The experimental time-resolved data clearly show two lifetimes and decay-associated spectra which must be assigned to such processes. The exact analytical formulae for these kinetics would be too complex for practical use. We therefore did not make an attempt to derive them here. The situation bears some formal similarity, however, to the case of C-phycocyanin for which we derived analytical expressions. As long as we are aware of the slight differences between these two cases we can arrive at least at some semiquantitative assignment of the AP 681 components by using the analytical formalism given in reference 7. Such an assignment is also facilitated by a comparison of the decay-associated spectra of AP 681 with those of AP 665. It seems that the states absorbing at the shortest wavelength decay with the shortest lifetime. Thus, the τ_1 component (23 ps) should be assigned both on the basis of its decay-associated spectrum and its lifetime to the relaxation within the exciton pair formed by $\alpha^{\text{AP-84}}/\beta^{\text{AP-84}}$. It is reasonable that the observed transfer time is slightly longer than in AP 665 because there are now only two such pairs present. The τ_2 component (66 ps) then would have to be assigned preferentially to the relaxation within the $\beta^{\text{AP-84}}/\alpha^{\text{APB}}$ pair on the basis of similar reasons. The long lifetime τ_3 reflects the decay of the equilibrated system. Thus, the decay-associated spectra and lifetimes of AP 681 can also be understood well on the basis of its special structure, i.e., both its differences and its similarities with AP 665. It cannot be excluded that the fluorescence kinetics of AP 681 could be even more complex than just three-exponential. A necessary requirement for a more detailed analysis would be a resolved x-ray structure, however.

For all three AP complexes studied in this work, we observed fast picosecond components in the fluorescence kinetics which are attributed to transitions between different exciton states. Fast transients in the range of several tens of picoseconds have been observed also recently by picosecond absorption spectroscopy in AP complexes (49), but the inherently lower signal/noise ratio in these measurements does not allow for as detailed an analysis as presented here. In contrast no fast components have been observed for the equivalent AP trimers from *Anacystis* AN 112 in a recent study (50). We think it is unlikely that the difference in our results arises entirely due to the origin of the AP from different organisms. However, we do not have an explanation for the failure to observe such fast components in reference 50. In that study a variable lifetime, ranging from 30 to 80 ps was observed in AP 681 (APC B in that work) across the emission spectrum. It is clear that several studies by other groups have failed to resolve fast kinetic components in phycobiliproteins which have been

observed clearly by other groups (for review see reference 6). In several cases the reason for the failure to detect these fast components can be traced back to unsuitable excitation and/or detection wavelengths, insufficient signal/noise ratio and/or insufficient time resolution of the equipment used. It may be of interest in this context that we were also unable to resolve the fast components when we used a detector which resulted only in an ~ 120 ps apparatus halfwidth in earlier experiments.

We would like to thank Mrs. A. Keil, Mrs. B. Kalka, Mrs. Cl. Nickel, Mr. U. Pieper, and Mr. H.-V. Seeling for their technical assistance. The CD spectra have been recorded on an instrument in the group of Prof. Snatzke, Ruhr-Universität Bochum.

Partial financial support from the Deutsche Forschungsgemeinschaft to A. R. Holzwarth and W. Wehrmeyer is gratefully acknowledged. We also thank Prof. K. Schaffner for his interest and support of this work.

Received for publication 20 June 1988 and in final form 5 September 1989.

REFERENCES

1. Bittersmann, E., W. Reuter, W. Wehrmeyer, and A. R. Holzwarth. 1988. Picosecond energy transfer kinetics in allophycocyanin aggregates from *Mastigocladus laminosus*. In *Photosynthetic Light-Harvesting Systems*. H. Scheer and S. Schneider, editors. de Gruyter, Berlin. 451–455.
2. Wehrmeyer, W. 1983. Organization and composition of cyanobacterial and rhodophycean phycobilisomes. In *Photosynthetic Prokaryotes*. G. C. Papageorgiou and L. Packer, editors. Elsevier Science Publishers BV, Amsterdam. 1–22.
3. Glazer, A. N. 1984. Phycobilisome: a macromolecular complex optimized for light energy transfer. *Biochim. Biophys. Acta*. 768:29–51.
4. Scheer H. 1982. Phycobiliproteins: molecular aspects of a photosynthetic antenna system. *Mol. Biol. Biochem. Biophys.* 35:7–45.
5. Holzwarth, A. R. 1986. Fluorescence lifetimes in photosynthetic systems. *Photochem. Photobiol.* 43:707–725.
6. Holzwarth, A. R. 1987. Picosecond fluorescence spectroscopy and energy transfer in photosynthetic antenna pigments. *Top. Photosynth.* 8:95–157.
7. Holzwarth, A. R., J. Wendler, and G. W. Suter. 1987. Studies on chromophore coupling in isolated phycobiliproteins. II. Picosecond energy transfer kinetics and time-resolved fluorescence spectra of C-phycocyanin from *Synechococcus* 6301 as a function of the aggregation state. *Biophys. J.* 51:1–12.
8. Wendler, J., W. John, H. Scheer, and A. R. Holzwarth. 1986. Energy transfer kinetics in trimeric C-phycocyanin studied by picosecond fluorescence kinetics. *Photochem. Photobiol.* 44:79–85.
9. Schirmer, T., W. Bode, R. Huber, W. Sidler, and H. Zuber. 1985. X-Ray crystallographic structure of the light-harvesting biliprotein C-phycocyanin from the thermophilic cyanobacterium *Mastigocladus laminosus* and its resemblance to globin structures. *J. Mol. Biol.* 184:257–277.
10. Schirmer, T., R. Huber, M. Schneider, W. Bode, M. Miller, and M. L. Hackert. 1986. Crystal structure analysis and refinement

- at 2.5 Å of hexameric C-phycoerythrin from the cyanobacterium *Agmenellum quadruplicatum*. The molecular model and its implications for light harvesting. *J. Mol. Biol.* 188:651–676.
11. Suter, G. W., and A. R. Holzwarth. 1987. A kinetic model for the energy transfer in phycobilisomes. *Biophys. J.* 52:673–683.
 12. Sidler, W., J. Gysi, E. Isker, and H. Zuber. 1981. The complete amino acid sequence of both subunits of allophycocyanin, a light harvesting protein-pigment complex from the cyanobacterium *Mastigocladus laminosus*. *Hoppe-Seyler's Z. Physiol. Chem.* 362:611–628.
 13. Rübli, R., M. Wirth, F. Suter, and H. Zuber. 1987. The phycobiliprotein beta-16.2 of the allophycocyanin core from the cyanobacterium *Mastigocladus laminosus*. Characterization and complete amino-acid sequence. *Biol. Chem. Hoppe-Seyler.* 368:1–9.
 14. Füglistaller, P., M. Mimuro, F. Suter, and H. Zuber. 1987. Allophycocyanin complexes of the phycobilisome from *Mastigocladus laminosus*. Influence of the linker polypeptide L 8.9c on the spectral properties of the phycobiliprotein subunits. *Biol. Chem. Hoppe-Seyler* 368:353–367.
 15. Lundell, D. J., and A. N. Glazer. 1981. A common beta subunit in *Synechococcus*: allophycocyanin B and allophycocyanin. *J. Biol. Chem.* 256:12600–12606.
 16. Lundell, D. J., and A. N. Glazer. 1983. Molecular architecture of light-harvesting antenna. Core substructure in *Synechococcus* 6301 phycobilisomes: two new allophycocyanin and allophycocyanin-b complexes. *J. Biol. Chem.* 258:902–908.
 17. Sauer, K., H. Scheer, and P. Sauer. 1988. Förster transfer calculations based on crystal structure data from *Agmenellum quadruplicatum* C-phycoerythrin. *Photochem. Photobiol.* 46:427–440.
 18. Sauer, K., and H. Scheer. 1988. Excitation transfer in C-phycoerythrin. Förster transfer rate and exciton calculation based on new crystal structure data for C-phycoerythrins from *Agmenellum quadruplicatum* and *Mastigocladus laminosus*. *Biochim. Biophys. Acta.* 936:157–170.
 19. Sauer, K., and H. Scheer. 1988. Energy transfer calculations for two C-phycoerythrins based on refined x-ray crystal structure coordinates of chromophores. In *Photosynthetic Light Harvesting Systems*. H. Scheer and S. Schneider, editors. de Gruyter, Berlin. 507–511.
 20. Schneider, S., C. Scharnagl, M. Duerring, T. Schirmer, and W. Bode. 1988. Effect of protein environment and excitonic coupling on the excited-state properties of the bilin chromophores in C-phycoerythrin. In *Photosynthetic Light Harvesting Systems*. H. Scheer and S. Schneider, editors. de Gruyter, Berlin. 483–490.
 21. Holzwarth, A. R., H. Lehner, S. E. Braslavsky, and K. Schaffner. 1978. Phytochrome models II: the fluorescence of biliverdin dimethyl ester. *Liebigs Ann. Chem.* 2002–2017.
 22. Levenberg, K. 1944. A method for the solution of certain non-linear problems in least squares. *Q. Appl. Math.* 2:164–168.
 23. Bevington, P. R. 1969. *Data Reduction and Error Analysis for the Physical Sciences*. McGraw Hill Book Co., New York. 1–336.
 24. Glazer, A. N. 1983. Comparative biochemistry of photosynthetic light-harvesting systems. *Annu. Rev. Biochem.* 52:125–157.
 25. Suter, F., P. Füglistaller, D. J. Lundell, A. N. Glazer, and H. Zuber. 1987. Amino-acid sequences of alpha-allophycocyanin-B from *Synechococcus* 6301 and *Mastigocladus laminosus*. *FEBS (Fed. Eur. Biochem. Soc.) Lett.* 217:279–282.
 26. Mörschel, E., K.-P. Koller, and W. Wehrmeyer. 1980. Biliprotein assembly in the disc-shaped phycobilisomes of *Rhodella violacea*. Electron microscopical and biochemical analyses of C-phycoerythrin and allophycocyanin aggregates. *Arch. Microbiol.* 125:43–51.
 27. Csatorday, K., R. MacColl, V. Csizmadia, J. Grabowski, and C. Bagyinka. 1984. Exciton interaction in allophycocyanin. *Biochemistry.* 23:6466–6470.
 28. Csatorday, K., R. MacColl, D. Guard-Friar, and C. A. Hanzlik. 1987. Excitation energy transfer between sensitizing chromophores of phycocyanin 612. *Photochem. Photobiol.* 45:845–848.
 29. Scheer, H. 1986. Excitation transfer in phycobiliproteins. In *Encyclopedia of Plant Physiology: Photosynthesis III*. L. A. Staehelin and C. J. Arntzen, editors. Springer-Verlag, Berlin. 19:327–337.
 30. Kobayashi, T., E. O. Degenkolb, R. Bersohn, P. M. Rentzepis, R. MacColl, and D. S. Berns. 1979. Energy transfer among the chromophores in phycocyanins measured by picosecond kinetics. *Biochemistry.* 18:5073–5078.
 31. Dagen, A. J., R. R. Alfano, B. A. Zilinskas, and C. E. Swenberg. 1986. Analysis of fluorescence kinetics and energy transfer in isolated alpha subunits of phycoerythrin from *Nostoc sp.* *Photochem. Photobiol.* 43:71–79.
 32. Switalski, S. C., and K. Sauer. 1984. Energy transfer among the chromophores of C-phycoerythrin from *Anabaena variabilis* using steady state and time-resolved fluorescence spectroscopy. *Photochem. Photobiol.* 40:423–427.
 33. Hanzlik, C. A., L. E. Hancock, R. S. Knox, D. Guard-Friar, and R. MacColl. 1985. Picosecond fluorescence spectroscopy of the biliprotein phycocyanin 612. Direct evidence for fast energy transfer. *J. Lumin.* 34:99–106.
 34. Förster, T. 1965. In *Modern Quantum Chemistry*. O. Sinanoglu, editor. Academic Press, Inc., New York. 1–137.
 35. Robinson, G. W. 1967. Excitation transfer and trapping in photosynthesis. *Brookhaven Symp. Biol.* 19:16–48.
 36. Knox, R. S. 1986. Trapping events in light-harvesting assemblies. Theory and modeling of excitation delocalization and trapping. In *Encyclopedia of Plant Physiology: Photosynthesis III*. L. A. Staehelin and C. J. Arntzen, editors. Springer-Verlag, Berlin. 19:286–298.
 37. Kenkre, V. M., and R. S. Knox. 1974. Theory of fast and slow excitation transfer rates. *Phys. Rev. Lett.* 33:803–806.
 38. Jung, J., P.-S. Song, R. J. Paxton, M. S. Edelstein, R. Swanson, and E. E. Hazen, Jr. 1980. Molecular topography of the phycocyanin photoreceptor from *Chroomonas* species. *Biochemistry.* 19:24–32.
 39. MacColl, R., K. Csatorday, D. S. Berns, and E. Traeger. 1980. Chromophore interactions in allophycocyanin. *Biochemistry.* 19:2817–2820.
 40. Bixon, M., and J. Jortner. 1969. Electronic relaxation in large molecules. *J. Chem. Phys.* 50:4061–4070.
 41. Jortner, J., and S. Mukamel. 1974. Radiationless transitions. *Int. Rev. Sci.* 1:327–388.
 42. Englman, R., and J. Jortner. 1970. The energy gap law for radiationless transitions in large molecules. *Mol. Phys.* 18:145–164.
 43. Holzwarth, A. R., K. Razi Naqvi, and U. P. Wild. 1977. Slow internal conversion between two close lying singlet states in a large molecule: azuleno[5, 6, 7-cd]phenalene. *Chem. Phys. Lett.* 46:473–476.
 44. Csatorday, K., D. Guard-Friar, R. MacColl, and D. S. Berns. 1988. The development of exciton migration routes for phycocyanin 645 and allophycocyanin. *Photochem. Photobiol.* 47:285–291.
 45. Canaani, O., and E. Gantt. 1980. Circular dichroism and polarized

-
- fluorescence characteristics of blue-green algal allophycocyanins. *Biochemistry*. 19:2950–2960.
46. Holzwarth, A. R., J. Wendler, K. Schaffner, V. Sundström, A. Sandström, and T. Gillbro. 1983. Picosecond kinetics of excited state relaxation in biliverdin dimethyl ester. *Isr. J. Chem.* 23:223–231.
47. Braslavsky, S. E., A. R. Holzwarth, E. Langer, H. Lehner, J. I. Matthews, and K. Schaffner. 1980. Phytochrome models. IV. Conformational heterogeneity and photochemical changes of biliverdin dimethylesters in solution. *Isr. J. Chem.* 20:196–202.
48. Braslavsky, S. E., A. R. Holzwarth, and K. Schaffner. 1983. Conformation analysis, photophysics and photochemistry of bile pigments. Bilirubin and biliverdin dimethyl esters and related linear tetrapyrroles. *Angew. Chem. Int. Ed. Engl.* 95:670–689.
49. Gillbro, T., A. Sandström, V. Sundström, R. Fischer, and H. Scheer. 1988. Picosecond time-resolved energy transfer kinetics within C-phycocyanin and allophycocyanin aggregates. *In Organization and Function of Photosynthetic Antennas*. H. Scheer and S. Schneider, editors. de Gruyter, Berlin. 457–467.
50. Maxson, P., K. Sauer, and A. N. Glazer. 1987. Fluorescence spectroscopy of allophycocyanin complexes from *Synechococcus* 6301 strain AN112. *In Organization and Function of Photosynthetic Antennas*. H. Scheer and S. Schneider, editors. de Gruyter, Berlin. 439–449.